



Science Arts & Métiers (SAM)

is an open access repository that collects the work of Arts et Métiers Institute of Technology researchers and makes it freely available over the web where possible.

This is an author-deposited version published in: <https://sam.ensam.eu>
Handle ID: <http://hdl.handle.net/10985/22659>

To cite this version :

Saman VAFADAR, Wafa SKALLI, Aurore BONNET-LEBRUN, Ayman ASSI, Laurent GAJNY -
Assessment of a novel deep learning-based marker-less motion capture system for gait study -
Gait & Posture - Vol. 94, p.138-143 - 2022

Any correspondence concerning this service should be sent to the repository

Administrator : scienceouverte@ensam.eu



Assessment of a novel deep learning-based marker-less motion capture system for gait study

Saman Vafadar^{1,a}, Wafa Skalli^{1,b}, Aurore Bonnet-Lebrun^{1,c}, Ayman Assi^{2,d}, Laurent Gajny^{1,*}

¹ Institut de Biomecanique Humaine Georges Charpak, Arts et Metiers, Institute of Technology, Paris, France.

² Faculty of Medicine, University of Saint-Joseph in Beirut, Beirut, Lebanon.

*Corresponding author: Laurent Gajny, laurent.gajny@ensam.eu

Abstract

Background. Marker-less systems based on digital video cameras and deep learning for gait analysis could have a deep impact in clinical routine. A recently developed system has shown promising results in terms of joint center position but has not been yet evaluated in terms of gait outcomes.

Research question. How does this novel marker-less system compare to a marker-based reference system in terms of clinically relevant gait parameters?

Methods. The deep learning method behind the developed marker-less system was trained on a dedicated dataset consisting of forty-one asymptomatic and pathological subjects each performing ten walking trials. The system could estimate the three-dimensional position of seventeen joint centers or keypoints (e.g., neck, shoulders, hip, knee, and ankles). We evaluated the marker-less system against a marker-based system in terms of differences in joint position (Euclidean distance), detection of gait events (e.g., heel strike and toe-off), spatiotemporal parameters (e.g., step length, time), kinematic parameters (e.g., hip and knee extension-flexion), and inter-trial reliability for kinematic parameters.

Results. The marker-less system was able to estimate the three-dimensional position of joint centers with a mean difference of 13.1 mm (SD = 10.2 mm). 99% of the estimated gait events were estimated within 10 milliseconds of the corresponding reference values. Estimated spatiotemporal parameters showed zero bias. The mean and standard deviation of the differences of the estimated kinematic parameters varied by parameter (for example, the mean and standard deviation for knee extension flexion angle were -3.0° and 2.7°). Inter-trial reliability of the measured parameters was similar to that of the marker-based references.

Significance. The developed marker-less system can measure the spatiotemporal parameters within the range of the minimum detectable changes obtained using the marker-based reference system. Moreover, except for hip extension flexion, the system showed promising results in terms of several kinematic parameters.

Keywords – human pose estimation, marker-less, gait analysis, convolutional neural network, deep learning.

1 Introduction

Marker-less motion capture systems have the potential to provide efficient, cost-effective, and easy-to-use motion capture devices [1]–[5] that may help spread the use of gait analysis for clinical applications. Meanwhile, Clark et al., [1] in a literature review demonstrated that the validity of depth cameras for most kinematic parameters was limited ($r < 0.75$) [5]. In recent years, digital video cameras combined with deep learning-based human pose estimation methods have demonstrated significant progress [6]–[9]. Most of these methods estimate the joint centers' three-dimensional or two-dimensional positions from digital images. These methods can be utilized with different camera configurations to develop marker-less systems for various applications such as occupational safety [10] and clinical gait analysis [2], [11].

Deep learning has recently attracted a lot of interest in the biomechanics community for marker-less motion capture. For instance, Cronin claims in a recent study that existing marker-less systems may already be suitable for some applications like coaching or rehabilitation [12]. In more detail, Ota et al., [2] assessed the validity and reliability of joint kinematics, using a deep learning-based human pose estimation called OpenPose [6], for bilateral squat and treadmill walking movements. Meanwhile, OpenPose could only estimate the two-dimensional position of joint centers. Kanko et al. [3], [4] assessed the performance of a marker-less system in terms of spatiotemporal and kinematic parameters, mainly for treadmill walking. The marker-less system consisted of eight digital video cameras and could estimate the three-dimensional position of several keypoints on the human body using deep learning-based human pose estimation methods.

Exploring the potential of using fewer cameras, we developed a marker-less system based on novel deep learning-based pose estimation methods [7] (<https://git.io/JVYos>), four digital cameras, and a new dataset (ENSAM dataset) for clinical gait study [11]. The pose estimation method was previously trained on Human3.6M [13]. The training set of the ENSAM dataset was utilized to fine-tune the pose estimation method via transfer learning [12]. This dataset was well suited for gait study while other existing datasets (e.g., [13]) were less effective for this objective due to the small number of subjects, errors introduced by placing markers on regular clothing, and their homogeneity (young asymptomatic adults). The ENSAM dataset contained the walking trials of thirty-one asymptomatic and pathological subjects. Biplanar X-ray images were acquired by the EOS system (EOS imaging, Paris, France) to reduce the errors related to marker misplacement [14], [15] in the synthetically generated annotations of joint centers and landmarks from the marker-based motion capture system. To our knowledge, this dataset was the first and only one collected by digital video cameras, a marker-based system, and a medical imaging system.

Evaluation of the proposed marker-less system was performed on the test set of the ENSAM dataset in terms of joint position differences indicating the Euclidean distance between the estimated and the marker-based value of joint centers. The mean joint position difference was 1.4 cm and demonstrated the potential of the marker-less system for gait analysis. Nonetheless, no clinically relevant gait parameter was compared against the marker-based reference system. In this study, after expanding our dataset from thirty-one to forty-one subjects, we assessed the performance of the marker-less system in terms of gait outcomes. In addition, we updated the pose estimation method to also estimate the three-dimensional position of toes.

2 Materials and methods

2.1 Extended ENSAM Pose dataset

The extension of the ENSAM dataset [11] was done following the exact same setup and experimental protocol, including biplanar X-rays acquisitions, motion capture with a marker-based (VICON system, Oxford Metrics, UK) and a custom marker-less system (see [11] for details), from thirty-one to forty-one subjects. The marker set for the marker-based system was based on [16], [17]. The frame rate of the cameras (Vicon and marker-less system) was 100 Hz, and the resolution of digital cameras was 1920 x 1080 pixels. It consisted of twenty-four asymptomatic adults, two adults with a spinal disorder and fifteen children or teenagers suffering from X-Linked Hypophosphatemia (XLH). All subjects or their parents signed an informed consent. Their inclusion in this study was approved by the relevant ethics committee (CPP 06036 and CPP 06001, Paris VI).

The marker-less system recorded only videos. The annotation data for these videos (test and training set) were generated synthetically using the marker-based and EOS data [14], [15]. The marker-based data were processed and cleaned (e.g., gap fillings) using VICON Nexus software. A two-step visual quality check was performed for the annotation of each subject's videos. First, for each gait trial and camera, the detected reflective markers were projected onto several video frames in the middle of the gait trial. We carefully checked if the projections lied within 2 pixels of the marker in video frames. This step would verify the synchronization and calibration of the marker-less system with the marker-based one. Second, for each gait trial, every 50 frames (0.5 seconds), the annotations (body landmarks) were projected to the four camera views. We checked all four views simultaneously if the landmarks were correctly placed.

The extended ENSAM dataset was then randomly split into train and test sets. The training set was used to fine-tune [12] the pose estimation method of the marker-less system which had already been trained on the Human3.6M dataset. Then, the performance of the marker-less system was assessed on the test set. The training set (~75 000 3D poses) consisted of twenty-five subjects (13 female, 12 male), who were on average 21 years old (range: 8 – 41), mean height was 160 cm (range: 123 – 188), mean body mass was 56 kg (range: 23 – 86), and mean body mass index was 21.0 kg/m² (range: 15.2 – 25.4). The test set (~48 000 3D poses) consisted of sixteen subjects (5 female, 11 male), who were on average 22 years old (range: 6 – 44), mean height was 162 cm (range: 126 – 199), mean body mass was 60 kg (range: 28 – 90), and mean body mass index was 21.9 kg/m² (range: 15.6 – 29.4). More details are provided in supplementary material.

2.2 Auxiliary dataset

This dataset consisted of sixty-six asymptomatic subjects (age range: 18–60 years; weight: 71.3±15 kg; height: 170±10 cm). The marker-based motion capture system (VICON system, Oxford Metrics, UK) consisted of seven cameras. The markers were positioned following the Plug-in-Gait method [16] and biplanar X-ray images were acquired using the EOS system in a standard static posture. Then, the subjects were asked to walk at their chosen comfortable speed. This dataset was used only as a-priori knowledge for the calculation of kinematic parameters using the marker-less system.

2.3 Human pose estimation method

In [11], the marker-less system estimated the three-dimensional position of fifteen body keypoints – head, neck, shoulders, elbows, wrists, pelvis, hips, knees, and ankles – for the ENSAM test set (more information on the definition of joint centers is provided in supplementary materials). In this study, we updated the pose estimation method to also estimate the position of toes. The estimated joint centers were further used to measure the clinically relevant spatiotemporal and kinematic gait parameters. The workflow of this study is shown in Figure 1.

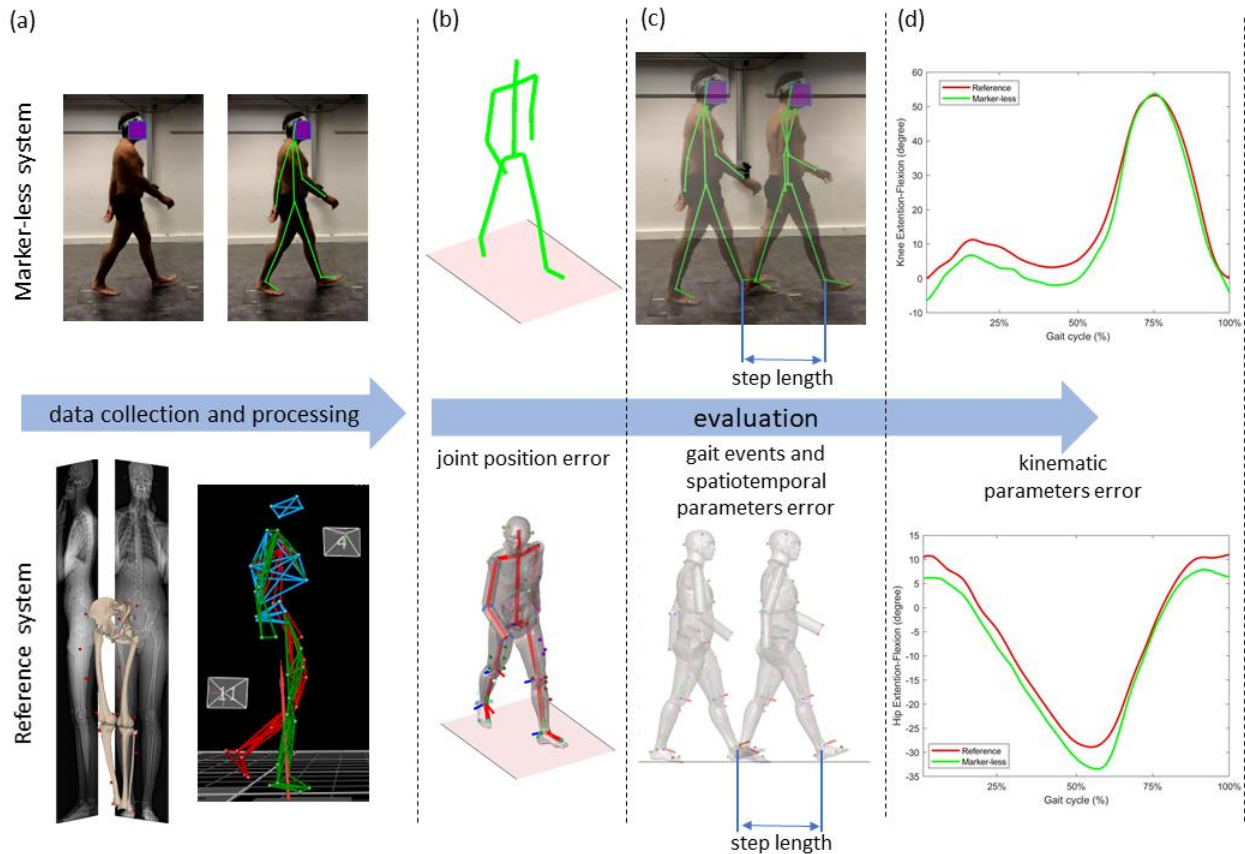


Figure 1. Workflow of study. (a) Data collection and processing by the marker-less (four colorful digital video cameras) and reference systems (a bi-plane X-ray image system and the VICON system); (b) Evaluation – joint position error as the Euclidean distance between the estimated three-dimensional joint centers and the corresponding reference values; (c) Evaluation – gait events and spatiotemporal parameters error as the difference between the estimated and corresponding reference parameters; (d) Evaluation – kinematic parameters error. The auxiliary dataset is used at only this level to help form the anatomical frames for the marker-less system.

2.4 Gait event detection and spatiotemporal parameters

Detection of heel strike and toe-off is essential for measuring spatiotemporal parameters. We estimated these gait events without force platforms. The gait event detection algorithm was adapted from [18], [19]. In [18], the algorithm was based on sacral and heel (or toe) markers' coordinates. We modified the algorithm to fit the marker-less system. The coordinates of the ankle and pelvis centers were used instead of the marker coordinates. Additionally, the joint centers were filtered using a zero-phase fourth-order Butterworth filter with the cutoff frequency of 7 Hz, as proposed in [19].

The measured spatiotemporal parameters were stride length (cm), gait speed (m/sec), step length (cm), step width (cm), step time (sec), stance time (sec), swing time (sec), cadence (steps/sec).

2.5 Kinematic parameters

The marker-less system estimated the three-dimensional position of body keypoints and for the derivation of gait analysis data, including kinematic parameters, no reference data (marker-based or EOS data) were incorporated. The marker-less system estimated two centers for each body segment – hip and knee centers for femur, knee and ankle centers for tibia. Therefore, the bony segments' anatomical frames were not mathematically observable and could not be determined. To resolve this issue, two different approaches were implemented.

First, a priori knowledge was incorporated to define the anatomical frames. For the anatomical frame of each body segment, an axis was directly determined by the data estimated by the marker-less system. For instance, for the pelvis anatomical frame, the Z-axis was defined as the line connecting the left and right hip joint centers. On the other hand, using the auxiliary dataset (subsection 2.1.2) and the Cardan convention [20], an average profile to represent the orientation of anatomical frames of the body segments with respect to the laboratory's global coordinate system is obtained for a single gait cycle. These average profiles were used as a priori knowledge of the orientation of the anatomical frames in the gait cycles. Therefore, to form an anatomical frame, for example for the pelvis, since the Z-axis was already obtained using the marker-less system, the Y-axis was approximated from the a priori knowledge to complete the anatomical frame. In this approach, the evaluated kinematic parameters are hip extension-flexion, knee extension-flexion, abduction-adduction and rotation of pelvis [21].

Second, two kinematic parameters, knee and ankle extension-flexion, were computed based on joint centers – called Joint-center Based (JB). JB knee extension-flexion is the angle between the vectors connecting the knee to the hip and the knee to the ankle. The JB ankle extension-flexion vectors were formed by connecting ankle to knee and ankle to toe.

2.6 Evaluation

The marker-less system estimated seventeen joint centers and keypoints for the sixteen subjects in the ENSAM test set. The differences in joint position, *i.e.*, the Euclidean distances between the estimates of joint centers from the marker-less and marker-based systems, were measured.

Concerning gait event detections, two tests were performed. First, the modified algorithm was used only for the marker-based system and compared to the original algorithm to assess the validity of this variant. Second, the modified algorithm was used for comparison between the marker-less and marker-based systems.

The evaluation metrics for assessing the agreement between the marker-less and the marker-based systems in terms of spatiotemporal and kinematic parameters, were the mean difference (bias), the standard deviation of difference, and the Bland-Altman 95% confidence interval limits of agreements.

The inter-trial reliability of kinematic parameters was also assessed using [22]. First, for each subject, the mean of the kinematic parameters over all walking trials was obtained. Then, the differences of parameters from the mean were computed for all walking trials. Thus, the inter-trial reliability was obtained by computing the standard deviation of the differences for all walking trials.

3 Results

3.1 Joint centers estimation

The differences in joint position are presented in Table 1. The ankles and shoulders were the joints with respectively the lowest (mean, 7.3 mm) and largest (mean, 18.5 mm) differences between the two systems. The mean position difference across all joints was 13.1 mm. Also, the 2SD and RMS values for the ankle were the lowest (2SD, 10.9; RMS, 9.1), the highest were for the wrists (2SD, 34.6; RMS, 23.6).

Table 1. Joint position error (mm) across all subjects of the extended ENSAM pose dataset.

Joint	toes	ankles	knees	hips	pelvis	neck	head	wrists	elbows	Shoulders
Mean	9.0	7.3	11.0	16.5	13.0	10.2	13.5	16.1	14.8	18.5
2SD	13.9	10.9	10.9	15.6	11.7	10.9	14.1	34.6	21.4	23.4
RMS	11.3	9.1	12.3	18.3	14.2	11.6	15.2	23.6	18.2	21.9

2SD: 2 standard deviation, RMS: root mean square

3.2 Gait event detection

In the first test, we compared the original and modified gait event detection algorithm only on the marker-based system. The mean difference between gait events was less than 1 millisecond demonstrating near-zero bias. The maximum difference was 20 milliseconds, and 98% of the differences were within 10 milliseconds.

In the second test, we implemented the modified algorithm to compare the agreement between the marker-less and the marker-based systems in detecting gait events. The mean differences, for all gait events, including right and left heel strike and toe-off, were less than 1 millisecond. 99% of gait events differences were within 10 milliseconds, and the maximum absolute difference was 20 milliseconds.

3.3 Spatiotemporal parameters

The difference between the spatiotemporal parameters measured by the marker-less and marker-based systems is presented in Table 2. The mean differences (biases) were close to zero. For example, the biases for stride length, step length, and step width were within 0.06 cm, and for step, stance, and swing time were within 1 millisecond.

Table 2. Difference between the spatiotemporal parameters determined using the marker-less and marker-based systems.

Parameter	MD	SD	LLoA	ULoA	MaxD
gait speed (m/sec)	0.00	0.00	-0.01	0.01	0.02
stride length (cm)	-0.06	0.81	-1.65	1.52	2.75
step length (cm)	-0.02	0.85	-1.69	1.64	3.00
step width (cm)	-0.04	0.39	-0.80	0.73	1.45
step time (msec)	0	6	-13	12	20
stance time (msec)	1	7	-13	15	20
swing time (msec)	1	7	-15	12	20
cadence (steps/sec)	0.00	0.02	-0.04	0.04	0.10

MD: mean difference, SD: standard deviation, LLoA: lower limit of agreement, ULoA: upper limit of agreement, MaxD: maximum difference

3.4 Kinematic parameters

The difference between the kinematic parameters measured by the marker-less and marker-based systems is presented in Table 3. The mean difference in the other kinematic parameters demonstrated a bias lower than 5° in absolute value. The biases for pelvis ab-adduction and JB parameters were limited to 1° or less. Considering the Normalized Standard Deviation (NSD), *i.e.*, standard deviation divided by the range of motion, of the kinematic parameters, knee extension-flexion showed the smallest deviation while pelvis ab-adduction showed the highest deviation.

Table 3. Difference (deg) between the kinematic parameters determined using the marker-less and marker-based systems.

Parameter	MD	SD	LLoA	ULoA	RoM	NSD
<i>pelvis ab-adduction</i>	-0.4	2.6	-5.6	4.7	4.0	0.65
<i>pelvis rotation</i>	2.9	2.8	-2.6	8.3	8.0	0.35
<i>hip extension-flexion</i>	4.5	8.2	-11.6	20.7	29.3	0.28
<i>Knee extension-flexion</i>	-3.0	2.7	-8.4	2.4	57.8	0.04
<i>JB knee extension-flexion</i>	-0.2	2.6	-5.2	4.9	56.2	0.05
<i>JB ankle extension-flexion</i>	1.1	4.7	-8.1	10.3	32.2	0.15

MD: mean difference, SD: standard deviation, LLoA: lower limit of agreement, ULoA: upper limit of agreement, RoM: range of motion, NSD: normalized standard deviation

3.5 Inter-trial reliability of kinematic parameters

The inter-trial reliability of the kinematic parameters, for both systems, is presented in Table 4. The maximum difference between the inter-trial reliability of marker-less and marker-based systems was 1.2°, which was for JB ankle extension-flexion. Except this parameter, the inter-trial reliability was similar.

Table 4. Inter-trial reliability (deg) of kinematic gait parameters

Parameter	Marker-less system	Marker-based system
<i>pelvis ab-adduction</i>	0.8	0.8
<i>pelvis rotation</i>	1.6	2.1
<i>hip extension-flexion</i>	1.4	1.3
<i>Knee extension-flexion</i>	2.6	2.5
<i>JB knee extension-flexion</i>	2.3	2.3
<i>JB ankle extension-flexion</i>	3.0	1.8

4 Discussion

In this study, we assessed a novel marker-less system introduced in [11] against a marker-based system in terms of clinically relevant spatiotemporal and kinematic gait parameters.

Gait event detection is of essential importance for determining gait cycles and measuring spatiotemporal gait parameters. Since we aimed to compare the marker-less system with the marker-based one, we modified and adapted a gait event detection algorithm [18] to be applicable for both systems. First, we assessed the modified algorithm, and demonstrated that the modifications caused negligible changes. Indeed, the mean difference between the modified algorithm and its original version was 1 millisecond,

and 98% of difference were less than 10 milliseconds. Then, we implemented the modified algorithm to compare the marker-less system against the marker-based one. The mean difference was 1 millisecond and 99% of differences were less than 10 milliseconds. Then, the spatiotemporal parameters were estimated based upon the detected gait events.

Performance evaluation of marker-less systems, in terms of spatiotemporal parameters, compared to marker-based systems can be accomplished using Minimum Detectable Changes (MDC) in spatiotemporal parameters measured by marker-based systems. MDC is the lowest change that identifies a true change exceeding the measurement error [23] and inherent variability of parameters. MDC values for spatiotemporal parameters have been measured for different populations, including children [24], healthy adults [25], older adults [26], people with chronic low back pain [27], and with Alzheimer’s disease [28], ranged from 0.12 to 0.17 m/sec for gait speed, 3 to 10 cm for stride length, 5 to 6 cm for step length, 2 to 3 cm for step width, 30 to 50 msec for step time, 30 to 70 msec for stance time, 30 to 40 msec for swing time, and 0.04 to 0.1 for cadence. The Bland-Altman lower and upper limits of agreement of spatiotemporal parameters were smaller than or equal to MDCs. For instance, the limits of agreement for step length were -1.69 cm and 1.64 cm, whereas the smallest MDC was 5 cm. Therefore, we conclude that the developed marker-less system can measure spatiotemporal parameters within the range of minimum detectable changes obtained using marker-based reference systems.

The agreement between the novel marker-less and marker-based systems was also studied in terms of kinematic parameters. In [29], the authors stated that errors less than 5° are “likely to be regarded as reasonable in gait analysis errors.” Assuming that 5° is the acceptable limit, the Bland-Altman limits of agreements for kinematic parameters showed that the difference between the marker-less system and the reference system for hip extension-flexion and JB ankle extension flexion is above the acceptable limit. However, pelvis ab-adduction and JB knee extension-flexion lied within this limit. Pelvis rotation and knee extension-flexion were close to be, but they were affected by a 3°-bias. This bias could be the result of the *a-priori* knowledge used when computing these parameters.

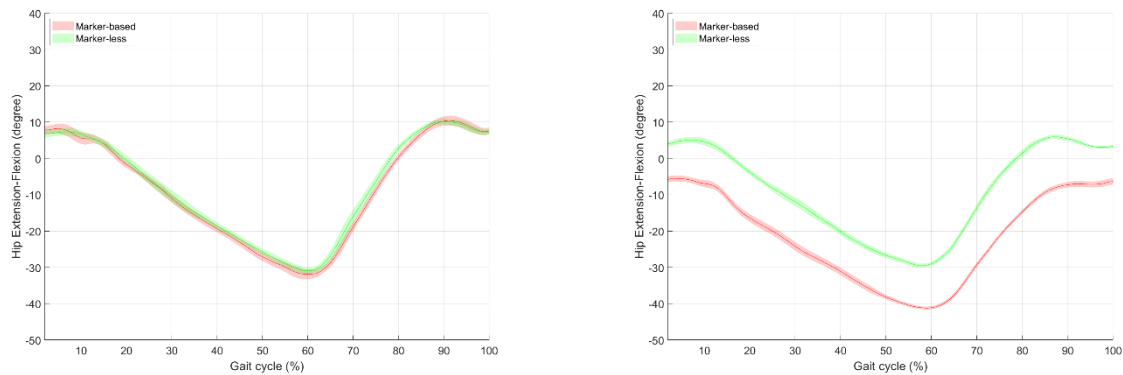


Figure 2. Hip extension-flexion measured by marker-less and marker-based systems for two different subjects across ten gait cycles. The lines and shaded bars represent respectively the mean and standard deviation values across ten gait cycles.

Kinematic parameters were computed based on anatomical frames and joint centers. For parameters based on anatomical frames, this inconsistency was generally due to the fact that the use of a mean axis for anatomical frame formation for all subjects resulted in a bias between marker-less and marker-based systems. For instance, Figure 2 shows hip extension-flexion measured by the marker-less and marker-based systems for two different subjects over 10 gait cycles. For one subject, the bias between the marker-

less and marker-based systems is much smaller than for the other. Knee extension-flexion and hip extension-flexion of all subjects of the ENSAM test set measured by the marker-less and marker-based systems are provided in the supplementary materials. In terms of joint center-based parameters, knee extension-flexion was almost within the acceptable limit of 5° (Bland-Altman limits of agreement were -5.2° and 4.9°), however, this was not true for ankle extension-flexion. For the latter, since one of the vectors is formed by connecting the ankle to toe, and these two centers, especially in children, are close to each other, even a small error in estimating the joint center resulted in a substantial error in ankle extension-flexion.

This study shows the potential of marker-less systems, based on digital video cameras and deep learning, for gait analysis in clinical applications. Meanwhile, the performance of the developed system is comparable to state-of-the-art marker-less systems [3], [4]. For instance, the root mean square difference for knee extension-flexion in our study was 4.1° , while in [3] it was 3.3° . Moreover, in terms of spatiotemporal parameters, both studies showed zero bias. The Bland-Altman limits of agreement for step length and swing time in [4] were 6.95 cm and 40 msec, whereas in our study they were 1.69 cm and 15 msec. It should be noted that the same method [18] was utilized for gait event detection in both studies. Despite similarities in the results, the developed marker-less systems had several differences. The number of cameras in our system was limited to four, compared to eight cameras. However, in our study, the training and test datasets were collected in the same laboratory environment. Finally, several subjects in our database did have gait disorders while in [3, 4], only healthy subjects were analyzed. As the results are encouraging, more effort should now be done to investigate various patterns of gait abnormalities.

This study has several limitations. First, the developed marker-less could estimate only two points for each body segment, for instance, the hip and knee joint centers for the thigh. Therefore, the anatomical frames are mathematically unobservable. We formed the anatomical frames by incorporating a priori knowledge on the movements of body segments that led to bias for kinematic parameters of some of the subjects and may fail in the case of severe gait disorder. Second, only the inter-trial reliability was investigated, while the reliability of a marker-less system should also be assessed by inter-session reliability. Work is underway to overcome these limitations. Regarding the first limitation, we may estimate a higher number of keypoints for each body segment or fit a multi-body model to the estimated keypoints. Third, marker-based systems are the reference systems for clinical gait analysis, but they do not provide ground truth data. The annotation data were generated synthetically using the marker-based and EOS data for the train or test set. Thus, the marker-less system, which learned to mimic the annotation data, also learned to mimic the soft-tissue artifact. Hence, the marker-less system outputs are still affected by the soft-tissue artifact. Finally, the ENSAM dataset, used for training and test, was collected in a single laboratory environment using one set of camera positions. Accordingly, for a single subject, consecutive three-dimensional poses were similar. Testing data from other environments are then required to appreciate the potential generalizability of this approach.

5 Conclusion

This study evaluated the developed marker-less motion capture system [11] in terms of clinically relevant spatiotemporal and kinematic gait parameters. The marker-less system was developed based on four digital video cameras, a deep learning-based human pose estimation method, and a dedicated dataset for gait study. It could estimate the three-dimensional position of seventeen joint centers with an average difference of 1.3 cm from the reference system. Evaluation of the marker-less system in terms of gait

outcomes demonstrated promising results. The marker-less system can measure the spatiotemporal parameters within the range of minimum detectable changes obtained by marker-based systems. Although the results indicated a lack of agreement for some kinematic parameters, in terms of inter-trial reliability, the marker-less system was as reliable as the marker-based system. This study is a proof-of-concept that shows the strong potential of marker-less systems for clinical gait analysis. Further studies are needed to investigate the applicability of the developed system for different gait pathologies and in various clinical environments.

6 Acknowledgments

The authors thank the ParisTech BiomecAM chair program, on subject-specific musculoskeletal modelling and in particular Société Générale and COVEA. The authors also thank Marc Khalifé, Mathis Renaudin and Amine Hamza for technical assistance.

7 References

- [1] R. A. Clark, B. F. Mentiplay, E. Hough, and Y. H. Pua, “Three-dimensional cameras and skeleton pose tracking for physical function assessment: A review of uses, validity, current developments and Kinect alternatives,” *Gait & Posture*, vol. 68, pp. 193–200, Feb. 2019, doi: 10.1016/j.gaitpost.2018.11.029.
- [2] M. Ota, H. Tateuchi, T. Hashiguchi, and N. Ichihashi, “Verification of validity of gait analysis systems during treadmill walking and running using human pose tracking algorithm,” *Gait & Posture*, vol. 85, pp. 290–297, Mar. 2021, doi: 10.1016/j.gaitpost.2021.02.006.
- [3] R. M. Kanko, E. K. Laende, E. M. Davis, W. S. Selbie, and K. J. Deluzio, “Concurrent assessment of gait kinematics using marker-based and markerless motion capture,” *Journal of Biomechanics*, vol. 127, p. 110665, Oct. 2021, doi: 10.1016/j.jbiomech.2021.110665.
- [4] R. M. Kanko *et al.*, “Assessment of spatiotemporal gait parameters using a deep learning algorithm-based markerless motion capture system,” *Journal of Biomechanics*, vol. 122, p. 110414, Jun. 2021, doi: 10.1016/j.jbiomech.2021.110414.
- [5] S. Springer and G. Yogeve Seligmann, “Validity of the Kinect for Gait Assessment: A Focused Review,” *Sensors*, vol. 16, no. 2, Art. no. 2, Feb. 2016, doi: 10.3390/s16020194.
- [6] Z. Cao, G. Hidalgo, T. Simon, S.-E. Wei, and Y. Sheikh, “OpenPose: Realtime Multi-Person 2D Pose Estimation using Part Affinity Fields,” *arXiv:1812.08008 [cs]*, May 2019, Accessed: Nov. 12, 2020. [Online]. Available: <http://arxiv.org/abs/1812.08008>
- [7] K. Isakov, E. Burkov, V. Lempitsky, and Y. Malkov, “Learnable Triangulation of Human Pose,” 2019, pp. 7718–7727. Accessed: Nov. 12, 2020. [Online]. Available: https://openaccess.thecvf.com/content_ICCV_2019/html/Isakov_Learnable_Triangulation_of_Human_Pose_ICCV_2019_paper.html
- [8] H. Qiu, C. Wang, J. Wang, N. Wang, and W. Zeng, “Cross View Fusion for 3D Human Pose Estimation,” 2019, pp. 4342–4351. Accessed: Nov. 12, 2020. [Online]. Available: https://openaccess.thecvf.com/content_ICCV_2019/html/Qiu_Cross_View_Fusion_for_3D_Human_Pose_Estimation_ICCV_2019_paper.html
- [9] N. B. Gundavarapu, D. Srivastava, R. Mitra, A. Sharma, and A. Jain, “Structured Aleatoric Uncertainty in Human Pose Estimation.,” in *CVPR Workshops*, 2019, vol. 2.
- [10] R. Mehrizi, X. Peng, X. Xu, S. Zhang, and K. Li, “A Deep Neural Network-based method for estimation of 3D lifting motions,” *Journal of Biomechanics*, vol. 84, pp. 87–93, Feb. 2019, doi: 10.1016/j.jbiomech.2018.12.022.

- [11] S. Vafadar *et al.*, “A novel dataset and deep learning-based approach for marker-less motion capture during gait,” *Gait & Posture*, vol. 86, pp. 70–76, May 2021, doi: 10.1016/j.gaitpost.2021.03.003.
- [12] N. J. Cronin, “Using deep neural networks for kinematic analysis: Challenges and opportunities,” *Journal of Biomechanics*, vol. 123, p. 110460, Jun. 2021, doi: 10.1016/j.jbiomech.2021.110460.
- [13] C. Ionescu, D. Papava, V. Olaru, and C. Sminchisescu, “Human3.6M: Large Scale Datasets and Predictive Methods for 3D Human Sensing in Natural Environments,” *IEEE Transactions on Pattern Analysis and Machine Intelligence*, vol. 36, no. 7, pp. 1325–1339, Jul. 2014, doi: 10.1109/TPAMI.2013.248.
- [14] X. Gasparutto, J. Wegrzyk, K. Rose-Dulcina, D. Hannouche, S. Armand, “The fusion of motion capture and 3D medical imaging for marker misplacements correction – a preliminary study,” *Gait & Posture*, vol. 73, pp. 572–573, Sep. 2019, doi: 10.1016/j.gaitpost.2019.07.296.
- [15] A. Assi *et al.*, “Validation of hip joint center localization methods during gait analysis using 3D EOS imaging in typically developing and cerebral palsy children,” *Gait & Posture*, vol. 48, pp. 30–35, Jul. 2016, doi: 10.1016/j.gaitpost.2016.04.028.
- [16] R. B. Davis, S. Öunpuu, D. Tyburski, and J. R. Gage, “A gait analysis data collection and reduction technique,” *Human Movement Science*, vol. 10, no. 5, pp. 575–587, Oct. 1991, doi: 10.1016/0167-9457(91)90046-Z.
- [17] A. Leardini, Z. Sawacha, G. Paolini, S. Ingrosso, R. Nativo, and M. G. Benedetti, “A new anatomically based protocol for gait analysis in children,” *Gait & Posture*, vol. 26, no. 4, pp. 560–571, Oct. 2007, doi: 10.1016/j.gaitpost.2006.12.018.
- [18] J. A. Zeni, J. G. Richards, and J. S. Higginson, “Two simple methods for determining gait events during treadmill and overground walking using kinematic data,” *Gait & Posture*, vol. 27, no. 4, pp. 710–714, May 2008, doi: 10.1016/j.gaitpost.2007.07.007.
- [19] C. M. O’Connor, S. K. Thorpe, M. J. O’Malley, and C. L. Vaughan, “Automatic detection of gait events using kinematic data,” *Gait & Posture*, vol. 25, no. 3, pp. 469–474, Mar. 2007, doi: 10.1016/j.gaitpost.2006.05.016.
- [20] A. Cappozzo, U. Della Croce, A. Leardini, and L. Chiari, “Human movement analysis using stereophotogrammetry: Part 1: theoretical background,” *Gait & Posture*, vol. 21, no. 2, pp. 186–196, Feb. 2005, doi: 10.1016/j.gaitpost.2004.01.010.
- [21] M. G. Benedetti *et al.*, “SIAMOC position paper on gait analysis in clinical practice: General requirements, methods and appropriateness. Results of an Italian consensus conference,” *Gait & Posture*, vol. 58, pp. 252–260, Oct. 2017, doi: 10.1016/j.gaitpost.2017.08.003.
- [22] M. H. Schwartz, J. P. Trost, and R. A. Wurvey, “Measurement and management of errors in quantitative gait data,” *Gait & Posture*, vol. 20, no. 2, pp. 196–203, Oct. 2004, doi: 10.1016/j.gaitpost.2003.09.011.
- [23] D. E. Beaton, “Understanding the Relevance of Measured Change Through Studies of Responsiveness,” *Spine*, vol. 25, no. 24, pp. 3192–3199, Dec. 2000.
- [24] S. C. McSweeney, L. F. Reed, and S. C. Wearing, “Reliability and minimum detectable change of measures of gait in children during walking and running on an instrumented treadmill,” *Gait & Posture*, vol. 75, pp. 105–108, Jan. 2020, doi: 10.1016/j.gaitpost.2019.10.004.
- [25] D. Meldrum, C. Shouldice, R. Conroy, K. Jones, and M. Forward, “Test–retest reliability of three dimensional gait analysis: Including a novel approach to visualising agreement of gait cycle waveforms with Bland and Altman plots,” *Gait & Posture*, vol. 39, no. 1, pp. 265–271, Jan. 2014, doi: 10.1016/j.gaitpost.2013.07.130.
- [26] M. Almarwani, S. Perera, J. M. VanSwearingen, P. J. Sparto, and J. S. Brach, “The test–retest reliability and minimal detectable change of spatial and temporal gait variability during usual over-ground walking for younger and older adults,” *Gait & Posture*, vol. 44, pp. 94–99, Feb. 2016, doi: 10.1016/j.gaitpost.2015.11.014.

- [27] R. Fernandes, P. Armada-da-Silva, A. Pool-Goudaazward, V. Moniz-Pereira, and A. P. Veloso, "Test–retest reliability and minimal detectable change of three-dimensional gait analysis in chronic low back pain patients," *Gait & Posture*, vol. 42, no. 4, pp. 491–497, Oct. 2015, doi: 10.1016/j.gaitpost.2015.08.002.
- [28] J. E. Wittwer, K. E. Webster, P. T. Andrews, and H. B. Menz, "Test–retest reliability of spatial and temporal gait parameters of people with Alzheimer’s disease," *Gait & Posture*, vol. 28, no. 3, pp. 392–396, Oct. 2008, doi: 10.1016/j.gaitpost.2008.01.007.
- [29] J. L. McGinley, R. Baker, R. Wolfe, and M. E. Morris, "The reliability of three-dimensional kinematic gait measurements: A systematic review," *Gait & Posture*, vol. 29, no. 3, pp. 360–369, Apr. 2009, doi: 10.1016/j.gaitpost.2008.09.003.